

## *Homotrema rubrum* (Lamarck) taphonomy as an overwash indicator in Marine Ponds on Anegada, British Virgin Islands

Jessica E. Pilarczyk · Eduard G. Reinhardt

Received: 15 March 2010 / Accepted: 11 December 2010 / Published online: 2 February 2011  
© Springer Science+Business Media B.V. 2011

**Abstract** Marine hypersaline ponds on Anegada, British Virgin Islands contain stratigraphic evidence (Shell and Sand Sheet) of a A.D. 1650–1800 overwash event that could have formed through a hurricane or tsunami. Candidates for the deposit include far-field (e.g. 1755 Lisbon tsunami) and local Puerto Rico Trench events (e.g. 1690), but hurricanes cannot be ignored. The goal of this study is to provide additional information to assess the origin of the deposit by examining the taphonomic characters of *Homotrema rubrum*, a common encrusting foraminifer in Caribbean reef settings. Surface samples ( $n = 12$ ) from major sub-environments (reef-flat, beach, storm wrack, and dune) and pond sections ( $n = 6$ ; 20–80 cm thick) are analyzed for their *Homotrema* concentration (specimens/cm<sup>3</sup>) and taphonomic character. Particle-size analysis was conducted on the same sections and samples. Highly Preserved (red colored, angular, intact chambers) *Homotrema* dominate the beach, storm wrack, and reef-flat deposits relative to the dune sand, but the beach and storm wrack contain the largest specimens. The Shell and Sand Sheet in the pond has Highly Preserved and abundant *Homotrema* (specimens/cm<sup>3</sup>) versus other sedimentary units in the ponds (e.g. Mud Cap and Shelly Mud). Its taphonomic character is most similar (test size and condition) to the storm wrack deposit on the beach indicating an outside provenance for the sand. Concentration of *Homotrema* in the Shell and Sand Sheet declined southward indicating a northerly reef-flat provenance for the overwash, although it does not preclude a southern inundation as well. It is unclear whether *Homotrema* individuals originated from the reef itself or were eroded from older beach ridge deposits during the overwash event. Conclusions from *Homotrema* taphonomic analysis were limited by the lack of comparative data from known hurricane and tsunami deposits in other Caribbean regions.

**Keywords** Foraminifera · Taphonomy · *Homotrema* · Storm · Tsunami · Gulf of Mexico

---

J. E. Pilarczyk (✉) · E. G. Reinhardt  
School of Geography and Earth Sciences, McMaster University, 1280 Main Street West,  
Hamilton, ON L8S 4K1, Canada  
e-mail: pilarcje@mcmaster.ca

E. G. Reinhardt  
e-mail: ereinhar@mcmaster.ca

## 1 Introduction

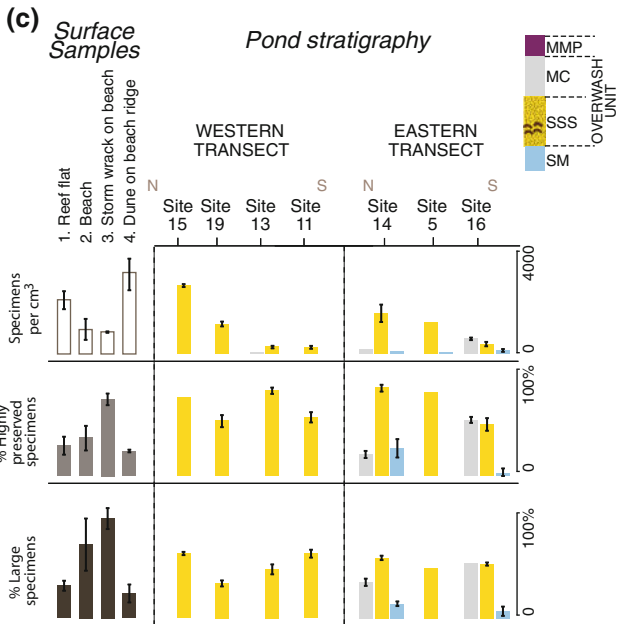
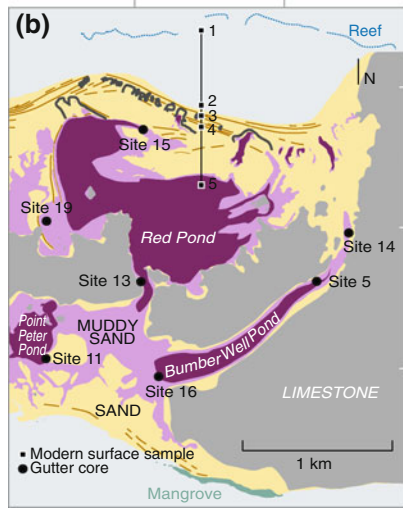
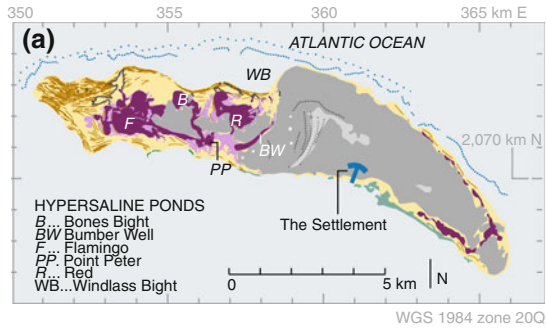
Marine ponds have proven to be excellent recorders of overwash events, with sandy deposits often ascribed to major storm events, although tsunamis are also a possibility (e.g. Donnelly 2005; Park et al. 2009). In the Caribbean, most overwash deposits are considered to be formed by hurricanes rather than tsunamis due to their frequency. However, there are several historical accounts of tsunamis affecting the Caribbean (e.g. 1755 Lisbon tsunami). These accounts are sparse and there are few comparative geological studies to assess the records (e.g. Atwater et al. 2010; Jones and Hunter 1992). Anegada, British Virgin Islands, due to its position relative to the Atlantic Ocean and the Puerto Rico Trench, may be a good tsunami recorder of local (e.g. 1690, 1867; Reid and Taber 1920; Zahibo et al. 2003) and trans-oceanic events (e.g. 1755 Lisbon; O’Loughlin and Lander 2003). However, potential tsunami overwash events are expected to be intermingled with hurricane deposits and discerning between the two maybe difficult. Modern hypersaline ponds on Anegada show a distinctive Shell and Sand Sheet that is laterally extensive and contains abundant foraminifera including *Homotrema rubrum* (Lamarck; Fig. 1). The origin of the overwash is not known as the chronologic (e.g. between A.D. 1650 and 1800) and stratigraphic evidence could not provide the necessary resolution to ascribe it to a known hurricane or tsunami (Atwater et al. 2010). The goal of this study is to provide additional data for assessing the deposit by determining the sand provenance using the taphonomy of *Homotrema* fragments.

Foraminiferal provenance is used extensively to document overwash events from both tsunamis and hurricanes (e.g. Hippensteel and Martin 1999; Scott et al. 2003; Hawkes et al. 2007; Mamo et al. 2009). However, there are few studies using taphonomic condition to help refine this data which could prove useful (e.g. Hawkes et al. 2007; Kortekaas and Dawson 2007). Taphonomic condition of the reef-dwelling *Homotrema rubrum* (Lamarck) has been shown to be an indicator of transport direction in reefal settings but has never been applied to overwash deposits (MacKenzie et al. 1965; Machado and Moraes 2002). It has great potential in this regard, as its encrusting habit in the reef provides a defined source for judging overwash dynamics.

### 1.1 *Homotrema rubrum* taphonomy

*Homotrema rubrum* (Lamarck) are red (bleaches to whitish-pink following death; Emiliani 1951), sessile foraminifera that grow attached to the lower surfaces of shells, corals, and reef detritus. The colored test consists of pronounced chambers that hollow after death (Fig. 2). *Homotrema* is restricted to latitudes between 30° N and 30° S, has a distribution similar to hermatypic corals, and is widely found in reef cryptic space, submarine caves and on non-growing areas of corals, reef rubble, shells, and calcareous algae (MacKenzie et al. 1965; Elliott et al. 1996 and references therein). Five test morphologies (hemispherical, globose, knobby, encrusting, and columnar) were initially related to environmental factors

**Fig. 1** **a**) Map of Anegada showing major geomorphic features (modified from Atwater et al. 2010). **b**) Detailed map of study area showing site locations of trenches (sites 5, 11, 13, 14, 15, 16, 19) and surface samples (1–5) depicted in (c). **c**) *Homotrema* taphonomic data from surface samples and major stratigraphic units in the ponds. Two north–south transects (western and eastern) are compared. The western transect runs through Red and Point Peter Ponds, while the eastern transect encompasses Bumber Well Pond. A generalized stratigraphic section based on all trench sections is indicated at the top right. *MMP* Microbial-Mat Peat, *MC* Mud Cap, *SSS* Shell and Sand Sheet, *SM* Shelly Mud



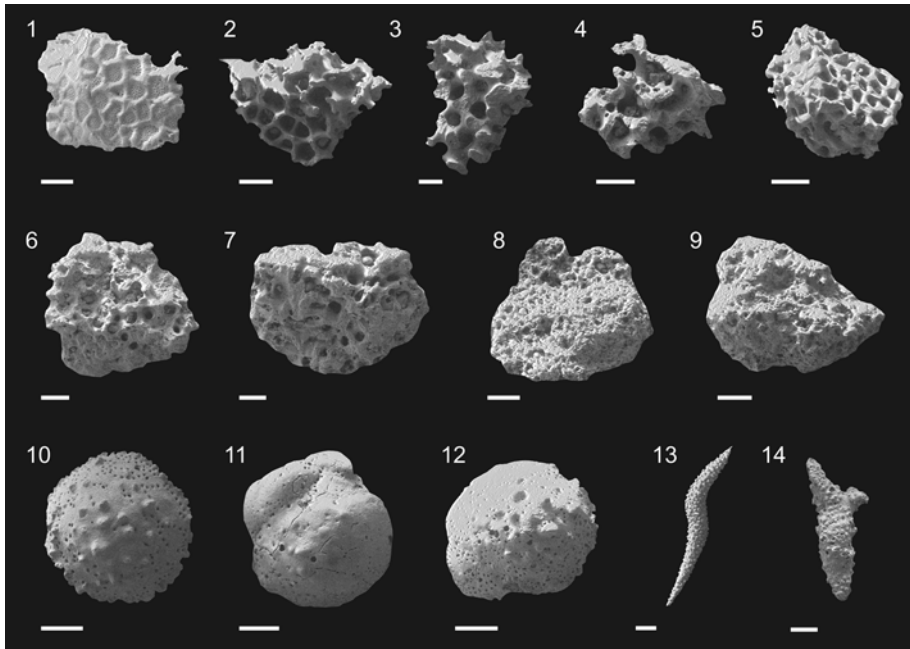


**Fig. 2** Taphonomic condition of *Homotrema* specimens. (1) Exceptionally preserved (red, angular, well preserved chambers); (2–5) Well preserved (pink, angular, hollowed chambers); (6–8) Moderately preserved (pink, rounded, hollowed chambers); (9) Highly altered (whitish, rounded, hollowed chambers); (10–12) *Homotrema* encrusted on *Ammonia beccari*, (10) Exceptionally preserved, (11) Well preserved (12) Moderately preserved; (13) Unaltered holothuridian spicule; (14) *Homotrema* encrusted holothuridian. Scale bars represent 100  $\mu\text{m}$

(Emiliani 1951) but later considered to be a result of both ontogeny and environment. Elliott et al. (1996) noted that test morphology was most affected by sedimentation, wave energy, light intensity, reproduction, competition, and predation, whereas knobby (branching) and globose tests dominated protected, less energetic habitats, and hemispherical and encrusting tests persisted in more energetic conditions.

MacKenzie et al. (1965) showed that *Homotrema* becomes detached with large waves and currents in the nearshore environment which disperses them over short distances from the reef. It was shown that the percentage of *Homotrema* decreased rapidly along a transect from the reefal zone inland toward the coastline. Beaches and more quiescent areas like open lagoons, often contained negligible abundances of *Homotrema*. Two of the three beaches analyzed by MacKenzie et al. (1965) contained small and well-rounded specimens of *Homotrema* compared to the larger more red specimens from the reef zone. Overall, the highest concentration of *Homotrema* occurred in the high-energy reef zone and decreased significantly closer to shore. It was concluded that *Homotrema* is a reliable indicator of sand transport dynamics in the reef system.

In a similar study, Machado and Moraes (2002) compared *Homotrema* from two reefal contexts with differing hydrodynamic settings. They found that well preserved, reddish specimens with angular edges were an indicator of proximity to their initial reefal context, whereas polished (rounded) specimens were evidence of sediment transport and/or energetic hydrological conditions.

## 2 Site description

Anegada, a small (54 km<sup>2</sup>) island part of the British Virgin Islands (BVI), is situated on the easternmost edge of the Caribbean unobstructed by the nearby islands to the north and east, making it ideal for detecting storm and tsunami overwash deposits (Fig. 1a). The Puerto Rico Trench, running parallel to Anegada's northern shore, is situated along the western side of a 1,300 km long subduction zone, where the North American plate is subducting under the Caribbean plate at a rate of 2 m per century (Lopez et al. 2006). The close proximity of the island to the trench (125 km away) and the open Atlantic make the island a potential recorder of local (e.g. 1867) and trans-oceanic tsunamis (e.g. 1755 Lisbon tsunami) as well as hurricanes.

A low-lying island, Anegada reaches maximum heights of 8 m above MSL (Mean Sea Level) on its western half (Atwater et al. 2010). Its northern windward coastline has a fringing reef that extends for 15 km to the southeast, while the leeward side of the island has a smaller system of patch reefs. An open lagoon extending ~1,000 m between the reef and Anegada's northern shore is characterized by a sandy reef flat with water depths ranging from 2–4 m. The ponds, located on the western side of the island, are confined by beach ridges that reach greater heights (2–4 m above MSL) on the windward side than they do on the leeward side. Numerous breaches of the beach ridges were recorded in aerial photographs and are interpreted in Atwater et al. (2010; Fig. 1a).

The hypersaline ponds (93–250 ppt; Jarecki and Walkey 2006), bounded by Pleistocene limestone highlands and beach ridges, are present on the western side of Anegada (Fig. 1a, b). Red pond is a small rounded basin that is situated closest to the windward side of the island. Bumber Well is elongate and contains an ephemerally flooded section along its northernmost tip. Point Peter is the smallest basin and is connected to Red Pond in the southeast. All 3 ponds have shallow water depths (~20 cm) and are capped with a microbial-mat peat that is dominated by cyanobacteria, diatoms, and sulphur bacteria in deeper layers (Jarecki and Walkey 2006).

## 3 Event history

Many Caribbean islands are hit annually by hurricanes but have unknown risks for local Puerto Rico Trench and trans-oceanic tsunamis (Atwater et al. 2010). Some known events include the tsunamis of 1690 and 1867 generated on the Puerto Rico Trench, although the precise epicentre remains unknown (Reid and Taber 1920; Stein 1982; McCann et al. 1984; Zahibo et al. 2003). Knowledge of these events is limited, but it was noted that the 1867 event would have reached Anegada from the south and resulted in wave heights ~1.5 m in Tortola, BVI (O'Loughlin and Lander 2003). Wave heights associated with the 1755 Lisbon tsunami were reported to reach 2–6 m at Hispaniola, Dominican Republic which is ~700 km to the west of Anegada, and on Cuba's coastline which is ~1,000 km WNW. However, there are no reports from Anegada as it was sparsely populated at the time (O'Loughlin and Lander 2003; Atwater et al. 2010).

Westward tracking hurricanes from the Atlantic Ocean were documented in the British Virgin Islands in 1713 (Pickering 1983), 1819 (Millás and Pardue 1968; Pickering 1983) and Hurricane Donna in 1960 (Dunn 1961). Donna was one of the largest (Category 3) hurricanes in the region in the last 50 years and attained wind speeds of 55 m/s. The eye of the storm came within 15 km of Anegada's southern shore, but eyewitness accounts report

that the storm surge only caused minor flooding in southern areas, (Dunn 1961; Atwater et al. 2010).

## 4 Methodology

### 4.1 Sample collection

Seven trench sections were recorded in Bumber Well, Red and Point Peter Ponds with gutter cores from sidewalls collected for detailed sampling (Fig. 1b). Surface samples were collected for comparative purposes from sub-environments: shallow reef-flat ( $n = 4$ ), beach ( $n = 3$ ), storm wrack deposits on beach ( $n = 3$ ), and dune sand on beach ridges ( $n = 2$ ; Fig. 1c). Radiocarbon dates from terrestrial organic matter and shells were performed at Woods Hole (NOSAMS; Fig. 3). Radiocarbon ages were calibrated using Calib (v 5.01, IntCal04 calibration data; Reimer et al. 2004) for terrestrial material and Marine04 (Hughen et al. 2004) for shells. Only calibrated ages (2 SD) are reported with further details provided in Atwater et al. (2010).

### 4.2 Taphonomic analysis

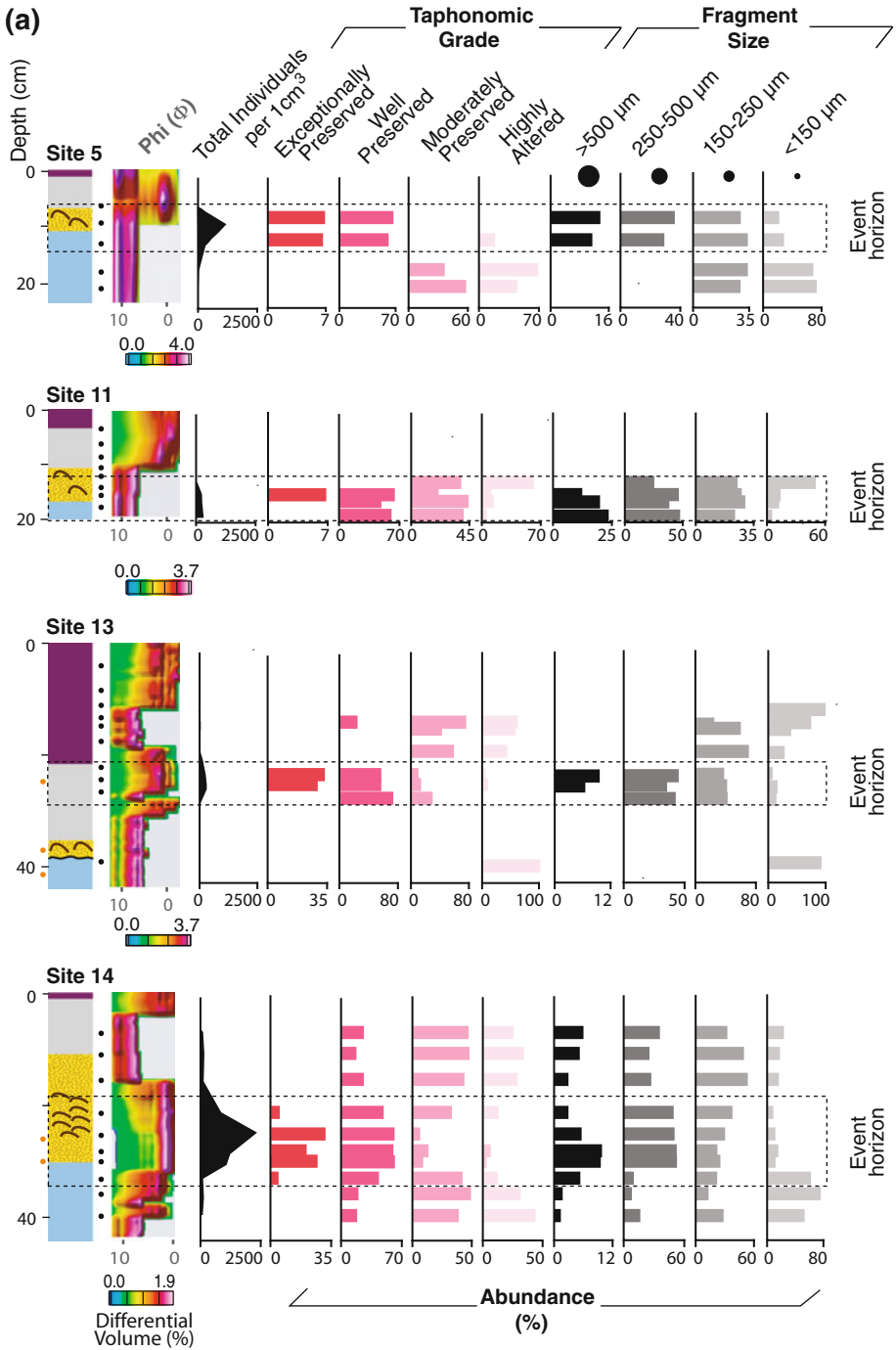
Approximately 1-cm<sup>3</sup> samples ( $n = 89$ ) were sieved ( $>63 \mu\text{m}$ ) and dried for taphonomic analysis (Fig. 3). Samples were subdivided with a dry splitter to provide specimen counts of  $\sim 300$  *Homotrema* and were identified and quantified using a binocular dissecting microscope ( $\times 60$ ). The number of *Homotrema* specimens per unit volume (specimens/cm<sup>3</sup>) was calculated for all samples. Scanning Electron Microscope (SEM) images of diagnostic specimens were taken using a Nikon Neoscope desktop SEM (Fig. 2).

Taphonomic preservation (Exceptionally Preserved, Well Preserved, Moderately Preserved or Highly Altered) and test size ( $>500 \mu\text{m}$ , 250–500  $\mu\text{m}$ , 150–250  $\mu\text{m}$  or  $<150 \mu\text{m}$ ) were recorded (Fig. 3). Tests that were red, angular, and contained a complete chamber structure were categorized as ‘Exceptionally Preserved’, while ‘Well Preserved’ tests were pink, angular, and had hollowed chambers. Rounded specimens that were pink with hollowed chambers were classified as ‘Moderately Preserved’, and those that were pink to white were classified as ‘Highly Altered’ (Figs. 1c, 3). For summary purposes in Fig. 1c, the Exceptionally and Well-Preserved categories are grouped into ‘Highly Preserved Specimens’ and specimens  $>250 \mu\text{m}$  are grouped into the ‘Large Specimens’ category.

### 4.3 Particle-size analysis (PSD)

Particle-size analysis was conducted on 6 cores using a Beckman Coulter LS230 laser diffraction particle size analyzer. Gutter cores were sampled at 1 cm resolution except Site 11 which was sampled at 1–2 cm. Samples were sieved (1,800  $\mu\text{m}$ ) before introduction into the LS230 as the instrument cannot analyze particle sizes  $>2,000 \mu\text{m}$ . Therefore, much of the shell material is not analyzed since many whole specimens are removed through sieving. Samples were homogenized by stirring as a moist paste before analysis

**Fig. 3** a) Detailed lithological, PSD, and *Homotrema* taphonomic data for core sites 5, 11, 13, 14, 15, 16, and 19. Event horizon designation is based on *Homotrema* concentration peak. Circles indicate sampling intervals (black) and radiocarbon dating intervals (orange; see Atwater et al. 2010 for details on the radiocarbon dates). b) Trench site locations for gutter cores. c) Generalized stratigraphic section based on all trench sections



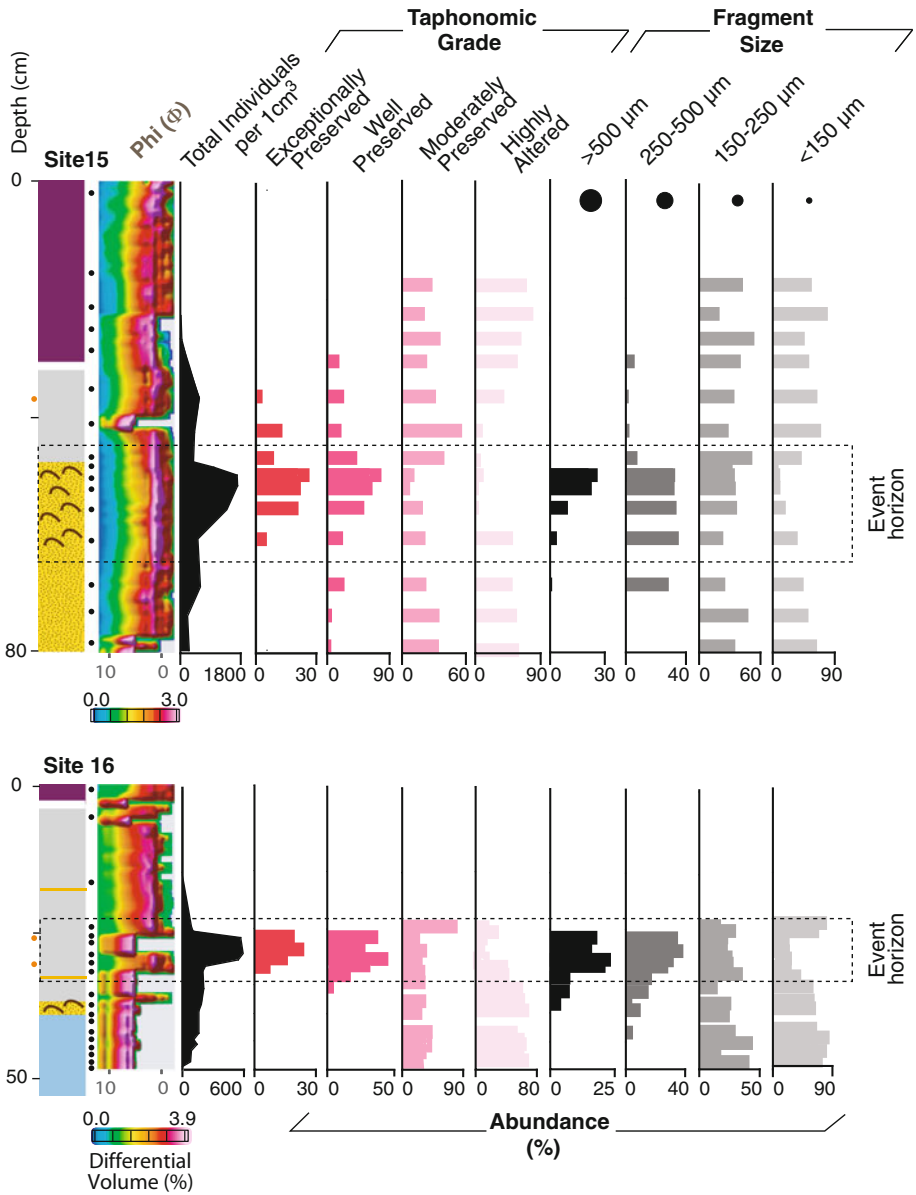


Fig. 3 continued



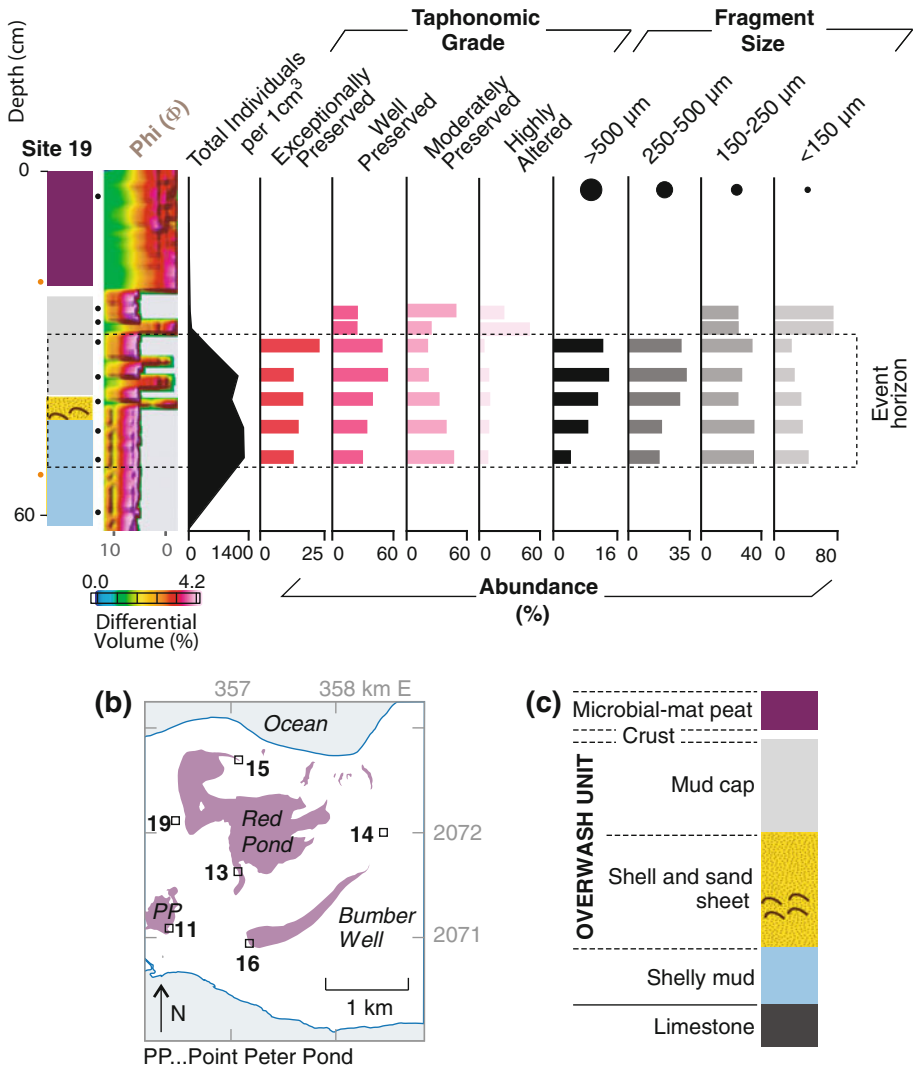
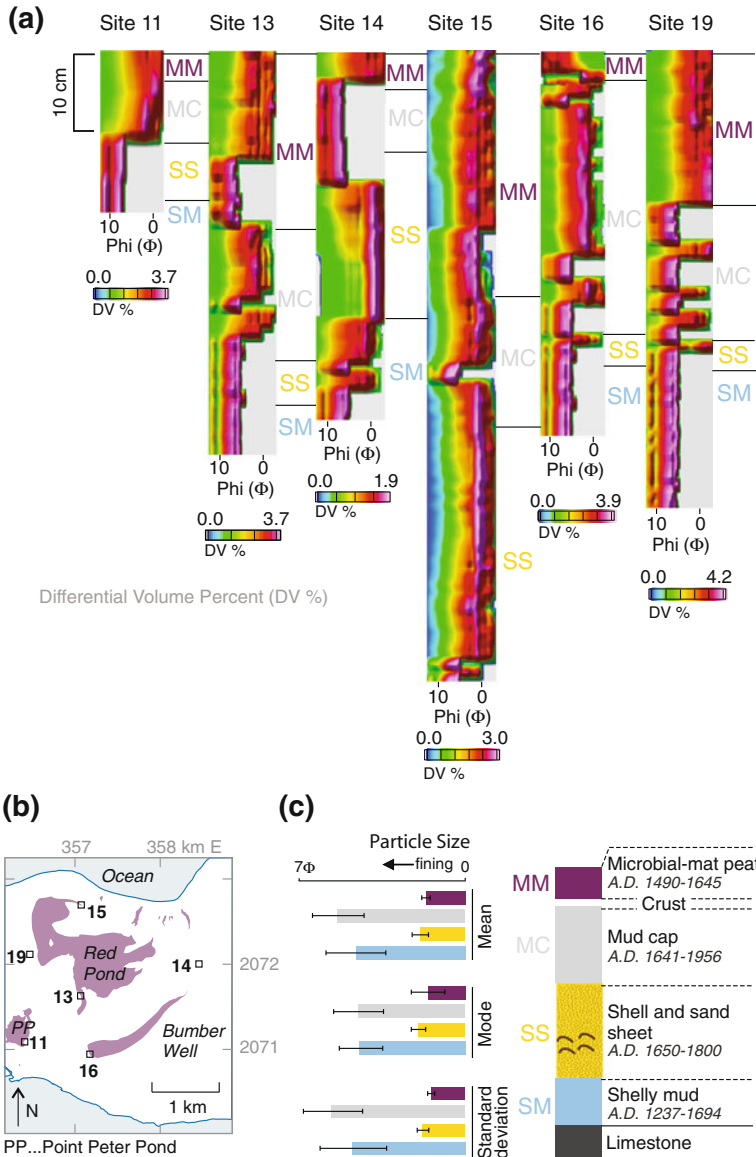


Fig. 3 continued

and ultrasonically disaggregated with hexametaphosphate ( $\text{NaPO}_3$ )<sub>6</sub> added to reduce flocculation. The Fraunhofer optical model was used to calculate particle-size distributions (Figs. 3, 4, 5). The particle-sizes were log transformed to the Wentworth Phi Scale, interpolated, and gridded using a triangular irregular network (TIN) algorithm (Sambridge et al. 1995) and plotted as color surface plots using Geosoft Oasis TM software (Donato et al. 2009; van Hengstum et al. 2007).



**Fig. 4** a) Core PSD plots for pond sections (gutter cores). Facies designations are based on field observations (see Fig. 3). b) Location of core sites (adapted from Atwater et al. 2010). c) Average PSD statistical data for facies

## 5 Results

### 5.1 Stratigraphy and particle-size distributions (PSDs)

Four distinct sedimentary units are found in the ponds as documented in Atwater et al. (2010). All trenches had basal limestone (likely Pleistocene; Howard 1970; Horsfield 1975)

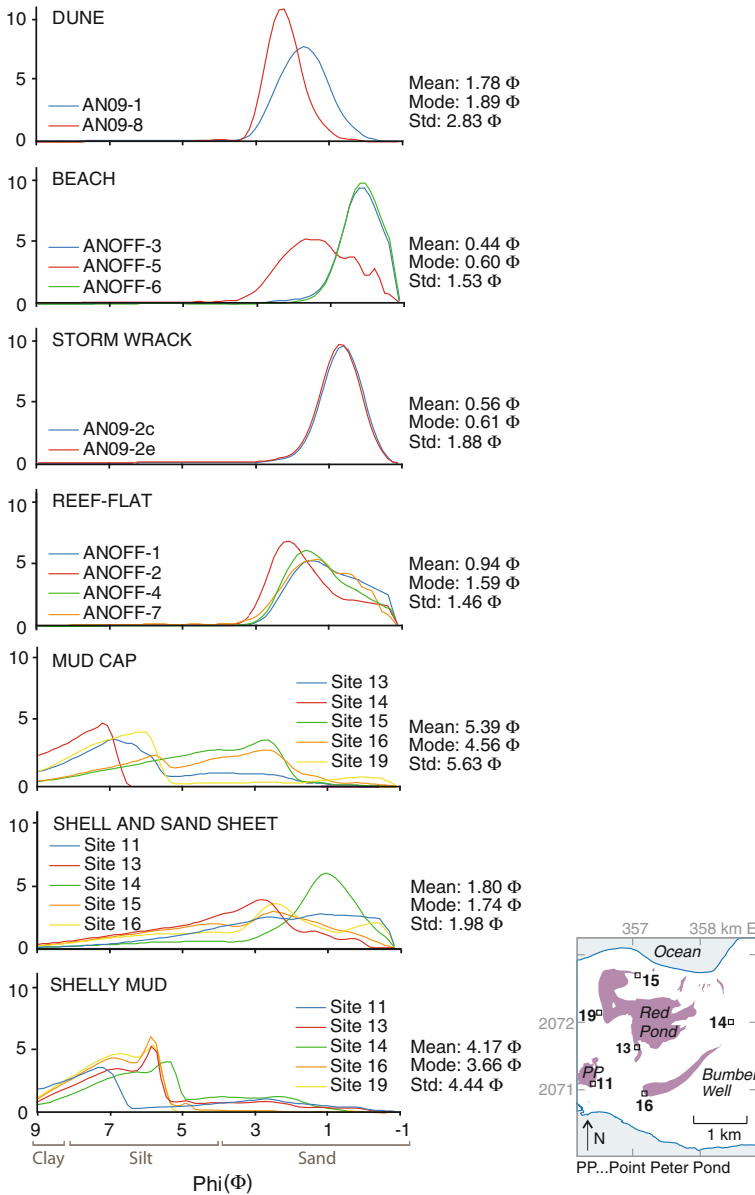


**Fig. 5** PSD plots of modern environments for comparison with the Mud Cap, Shell and Sand Sheet and Shelly Mud from pond stratigraphy. Statistical data (mean, mode, and SD) of each environment (*modern samples*) and unit (*core samples*) is indicated

with overlying units of Shelly Mud, a Shell and Sand Sheet, and a Mud Cap that sharply or gradationally transitioned to a microbial-mat peat (Figs. 4, 5). This stratigraphic succession was repeatedly found in trenches throughout the ponds (see Atwater et al. 2010), but it did vary somewhat from location to location (e.g. texture and thickness; Fig. 4c). Field

descriptions of the units were largely defined through the shell concentration and relative proportions of sand and lime mud.

The basal Shelly Mud is a 10–40 cm thick, massive, silty-clay sized, limey mud which was found in all three ponds (mean = 4.6  $\phi$ ; mode = 4.4  $\phi$ ; SD = 4.7  $\phi$ ; Figs. 3, 4, 5). Shell material in this mud was relatively low at 2 clasts/cm<sup>3</sup> and includes *Anomalocardia* spp. and cerithid gastropods, indicating a marine to hypersaline pond environment (Reinhardt et al. 2011). The foraminifera from this unit are predominately miliolids (~70% *Quinqueloculina* spp. and *Triloculina* spp.), which also typify coastal lagoons and marine ponds (Poag 1981; Murray 1991; Brewster-Wingard and Ishman 1999). The Shelly Mud is a well-defined stratigraphic unit in the ponds with characters that are found in all sections except Site 15. The PSD is skewed towards finer particle sizes, and the mode has two distinct peaks with an additional small peak in the fine tail of the PSD (Sites 13, 14, 16, 19). Very little sand is present suggesting isolation from outside reef-flat sources. The boundary between the overlying Shell and Sand Sheet does not always correspond with stratigraphic boundaries identified in the field (e.g. Site 14 could be 10 cm lower).

The Shell and Sand Sheet is heterogeneous in its composition. Although analyzed sites are predominantly from shallow margins of the ponds and contain shells and *Homotrema* sand, the sand was also found in central regions of each pond (Atwater et al. 2010). The unit (2–19 cm thick) is not well defined in the PSD data due to its variable characteristics in the pond and the removal of large shell material for analysis. It was well defined in the field sections due to the high concentration of clasts (shell and lithoclasts) and/or distinctive pink-colored sand (Atwater et al. 2010). Based on PSD data, the unit is (except Site 15) sand-sized but often contains a significant mud matrix (mean = 1.7  $\phi$ ; mode = 2.0  $\phi$ ; SD = 2.2  $\phi$ ; Figs. 3, 4, 5). The high bio-lithoclast concentration (6 clasts/cm<sup>3</sup>) includes shells, *Anomalocardia* spp. (bivalve) and cerithids (gastropod), with lithoclasts (pebbles). The clasts were derived from scour or winnowing of underlying Shelly Mud (Reinhardt et al. 2011). The fine to medium bioclastic sand contains abundant *Homotrema* and is generally well sorted but also contains a muddy matrix in many areas (Figs. 4, 5). In locations where small shell fragments and sand (<2 mm) are present, the PSD data corresponds well with the Shell and Sand sheet identified in the field (e.g. Site 14; Fig. 4); however, in units that contain larger shell material with muddy matrix, the correspondence was poor (e.g. Site 13; Fig. 4). The PSD distributions are not peaked compared to the other units likely reflecting a combination of pond and outside sourced sediment (Fig. 4). Trends in the PSD within the Shell and Sand Sheet are not well defined perhaps due to the missing >2 mm clasts in the analysis; however, slight trends are present in the field defined intervals but vary from normal to reverse grading.

The Mud Cap is a lime mud that transitions to a Microbial-Mat Peat, which presently covers the modern pond surface. The unit ranges in thickness from 1–30 cm as defined by field logging of trench sections. Particle sizes are variable in the unit, but typically are mud to sandy mud (mean = 3.8  $\phi$ ; mode = 3.9  $\phi$ ; SD = 3.7  $\phi$ ; e.g. Site 14 vs. Site 16) and contain interspersed sandy laminae (e.g. Site 19). The PSD of this unit is most similar to the Muddy Shell of the former marine pond; however, the PSDs are not entirely consistent (Figs. 4c, 5) suggesting that it was deposited under different conditions. Often there is little PSD distinction between what is defined as the Shell and Sand Sheet and the Mud Cap (Fig. 3). Atwater et al. (2010) considers the Shell and Sand Sheet and the Mud Cap to be from the same event that may explain the poorly defined boundaries. The difference between the two is largely in the concentration of >2 mm clasts which is lower in the Mud Cap at 2 clasts/cm<sup>3</sup> versus 6 clasts/cm<sup>3</sup> in the Shell and Sand Sheet (Reinhardt et al. 2011).

The clast composition is very similar to the Shelly Mud and the Shell and Sand Sheet (i.e. all *Anomalocardia* and cerithids; Reinhardt et al. 2011).

The transition to the microbial-mat peat is either distinct with a carbonate crust (Atwater et al. 2010) or gradual and hard to define. It ranges in thickness from 1–22 cm and contains the largest particle-sizes of any unit (mean = 1.6  $\phi$ ; mode = 1.6  $\phi$ ; SD = 1.4  $\phi$ ), a reflection of the presence of evaporite crystals in the mats. However, the PSD analyses also include particles of algal mats so the values are not entirely accurate.

## 5.2 *Homotrema* taphonomy

The modern surface samples collected from various sub-environments have distinctly different characteristics. The highest concentration of *Homotrema* is in the dune sand ( $3,503 \pm 1,414$  specimens/cm<sup>3</sup>), followed by the reef-flat ( $2,710 \pm 966$ ), beach ( $1,060 \pm 950$ ), storm wrack deposit ( $848 \pm 50$ ) and hypersaline pond ( $354 \pm 393$ ; Fig. 1c). The most altered *Homotrema* are found in the dune sand with only  $24 \pm 3\%$  Highly Preserved specimens which are small ( $21 \pm 15\%$  in large size fraction). The largest and the best preserved specimens are found in the storm wrack deposits ( $75 \pm 17\%$ ;  $66 \pm 10\%$ ), the beach ( $63 \pm 44\%$ ;  $37\% \pm 24$ ) and the reef-flat ( $32 \pm 10\%$ ;  $34 \pm 20\%$ ).

In all the analyzed pond sections, there is a prominent peak in *Homotrema* concentration (specimens/cm<sup>3</sup>) that generally coincides with the Shell and Sand Sheet from the field observations. The exception was in Sites 13 and 16 where there is a peak in the Mud Cap (Figs. 1c, 3). Atwater et al. (2010) associates the Mud Cap with the overwash event itself, which may explain the *Homotrema* peak in the mud. The specimens associated with the *Homotrema* peak are predominantly large (i.e. >250  $\mu$ m), Highly Preserved (i.e. exceptionally to well preserved) with red to dark-pink color and many intact chambers (Figs. 1c, 2, 3). They closely match the modern beach, reef-flat, and storm wrack deposits and therefore are indicative of overwash. Above and below this peak, large and Highly Preserved *Homotrema* specimens are absent at most sites (e.g. 5, 11, 13, 16 and 19). The lack of Highly Preserved specimens in the Shelly Mud indicates it is not a source for the *Homotrema* in the Shell and Sand Sheet like it is for the >2 mm clasts (Reinhardt et al. 2011). Smaller (<150–250  $\mu$ m), moderately to highly altered specimens are found (10–90%) in low concentrations in both the underlying Shelly Mud and also the overlying Mud Cap, but not in all instances (e.g. Site 16 vs. Site 14; Fig. 3). These specimens are likely aeolian sand inputs from surrounding dunes as the taphonomic condition is a close match.

The concentration of *Homotrema* tests (specimens/cm<sup>3</sup>) in the Shell and Sand Sheet decreases markedly in the pond transects indicating a southerly trending overwash direction (Fig. 1c). The western transect through Red and Point Peter Ponds shows a southward decrease from  $2,714 \pm 59$  specimens/cm<sup>3</sup> at Site 15, to  $1,182 \pm 138$ ,  $284 \pm 51$  and  $264 \pm 34$  at Sites 19, 13 and 11, respectively. This southward decline likely represents a distance to source relationship with production of *Homotrema* occurring on the northern fringing reef, while the smaller patch reefs to the south would not produce as many individuals. It therefore does not preclude an additional inundation from the south (Reinhardt et al. 2011). Trends in other taphonomic characters are less prominent with proportions of large and Highly Preserved specimens showing taphonomic uniformity across the sheet deposit (Fig. 1c).

## 6 Discussion

Based on the stratigraphic data presented in Atwater et al. (2010), the Shell and Sand Sheet formed during an overwash event between A.D. 1650–1800, although the exact cause (tsunami vs. hurricane) is uncertain. The sheet-like geometry of the overwash deposit can be indicative of a tsunami (e.g. Morton et al. 2007) and the *Homotrema* data supports an outside provenance for the sand, which would strengthen this interpretation, but the lack of large (>2 mm) reef-flat clasts needs to be considered (Reinhardt et al. 2011).

The Shell and Sand Sheet has distinctive *Homotrema* taphonomy and closely matches outside sources (beach, storm wrack, and reef-flat). The storm wrack is an important deposit as its taphonomic signature is what might be expected from sorting and transport of reef-flat sediment during an overwash into the ponds. It contains high concentrations of Highly Preserved specimens, which is very similar to the Shell and Sand Sheet with abundant, large and Highly Preserved *Homotrema*. The decreasing concentration of *Homotrema* in the transects also indicates overwash from the north. However, the Shell and Sand Sheet is missing the coarse (>2 mm) reef-flat shell material that was a dominant component in the storm wrack deposit (Reinhardt et al. 2011). The lack of coarse reef-flat clasts suggests that the overwash sand originated from a combination of previously sorted deposits (i.e. beach) and/or reef-flat material that was sorted during the event itself.

Hydrodynamic modelling of possible tsunami scenarios and hurricanes (Category 5) indicates that only Lisbon (1775—Mw 9.0) or a Puerto Rico Trench (Mw 8.7, Mw 8.0) tsunami could cause the necessary inundation with a 2.25 m beach ridge elevation (Wei et al. 2010). The models show that hurricane waves tend to dissipate on the fringing reef and do not produce the necessary inundation. Buckley et al. (2011) model transport of boulders associated with the Shell and Sand Sheet and found that only a near-field Mw 8.0 Puerto Rico Trench outer-rise tsunami could move the boulders. The modeled tsunami inundations barely overtop the 2.25 m high beach ridges and if correct, may explain the lack of large reef-flat clasts in the Shell and Sand Sheet. A probable scenario involves entrainment of reef-flat and beach sediments with the coarse clasts left behind due to reducing flow competence as the inundation overtops the beach ridges. Plunge pools on the inner edge of the ponds may have also been a source of *Homotrema* as the scour may have eroded older beach deposits (Atwater et al. 2010).

Sandy overwash is a characteristic feature of hurricane deposits, but the sand bodies tend to be lobate in shape rather than sheet-like (e.g. Morton et al. 2007). Other studies of sandy overwash from Caribbean hurricanes only report sand and do not mention coarser reef clasts or *Homotrema* and therefore may not have been significant in those contexts (e.g. Donnelly 2005). However, this lack of comparative data makes it difficult to assess the results from Anegada. Anegada's ponds, with their close proximity to reef source regions and their low-lying topography, make it difficult to distinguish hurricane versus tsunami deposits. Here, we present plausible evidence that seems to support a tsunami interpretation, but further research is needed to constrain *Homotrema* taphonomic processes. Further analysis of other known hurricane and tsunami deposits is also required to better constrain differences in their signatures (e.g. MacKenzie et al. 1965; Machado and Moraes 2002).

## 7 Conclusions

*Homotrema* taphonomy shows promise as an overwash indicator for Caribbean reef environments. *Homotrema* are small (sand-sized), readily transported and have high

productivities, so are abundant in the sediment record (100–1,000/cm<sup>3</sup>). They have a defined provenance in the reef with known life-habits (attached) and quickly inherit taphonomic characteristics after death (e.g. bleaching of color). They are also visible in field observations due to their distinctive pink color and can be efficiently analyzed for high-resolution studies.

*Homotrema* taphonomy indicated overwash into Anegada's ponds that occurred from A.D. 1650–1800; however, it alone could not determine whether it formed from a tsunami or hurricane. Additional evidence from hydrodynamic modelling of the overwash event and boulder transport in the ponds suggests that it was from a tsunami rather than a hurricane. Conclusions from the *Homotrema* taphonomy were limited by the lack of comparative data from known hurricane and tsunami deposits. However, with future research, it may allow us to better understand the hydrodynamics of these events.

**Acknowledgments** The government of the British Virgin Islands permitted access to Anegada's salt ponds, use of airphotos, and guidance from its specialists in disaster management, surveying, and natural science. Among them, we especially thank Cynthia Rolli, Rondell Smith, Shannon Gore, and Dylan Penn. Lianna Jarecki shared her comprehensive knowledge of Anegada's salt ponds, Alejandra Rodriguez assisted with field work and Alyson Brown helped with laboratory work. Insightful comments from Brian Atwater and two anonymous reviewers greatly improved this manuscript. The work was supported in part by the Nuclear Regulatory Commission under its project N6480, a tsunami-hazard assessment for the eastern United States and an NSERC Discovery grant to ER.

## References

- Atwater BF, ten Brink US, Buckley M, Halley RS, Jaffe BE, Lopez-Venegas AM, Reinhardt EG, Tuttle MP, Watt S, Wei Y (2010) Geomorphic and stratigraphic evidence for an unusual tsunami or storm a few centuries ago at Anegada, British Virgin Islands. *Nat Hazards*. doi:10.1007/s11069-010-9622-6
- Brewster-Wingard GL, Ishman SE (1999) Historical trends in salinity and substrate in Central Florida Bay: a paleoecological reconstruction using modern analogue data. *Estuaries* 22:369–383
- Buckley M, Wei Y, Jaffe J, Watt S (2011) Inverse modeling of velocities and inferred cause of overwash that emplaced inland fields of boulders at Anegada, British Virgin Islands. *Nat Hazards*. doi:10.1007/s11069-011-9725-8
- Donato SV, Reinhardt EG, Boyce JI, Pilarczyk JE, Jupp BP (2009) Particle-size distribution of inferred tsunami deposits in Sur Lagoon, Sultanate of Oman. *Mar Geol* 257:54–64
- Donnelly J (2005) Evidence of past intense tropical cyclones from backbarrier salt pond sediments: a case study from Isla de Culebrita, Puerto Rico, USA. *J Coast Res* 42:201–210
- Dunn GE (1961) The hurricane season of 1960. *Mon Weather Rev* 89:99–108
- Elliott JM, Logan A, Thomas MLH (1996) Morphotypes of the foraminiferan *Homotrema rubrum* (Lamarck): distribution and relative abundance on reefs in Bermuda. *Bull Mar Sci* 58:261–276
- Emiliani C (1951) On the species *Homotrema rubrum* (Lamarck). *Cushman Found Foram Res Spec Cont* 2:143–147
- Hawkes AD, Bird M, Cowie S, Grundy-Warr C, Horton BP, Tan Shau Hwai A, Law L, Macgregor C, Nott J, Eong Ong J, Rigg J, Robinson R, Tan-Mullins M, Tiong T, Yasin Z, Wan Aik L (2007) Sediments deposited by the 2004 Indian Ocean tsunami along the Malaysia–Thailand Peninsula. *Mar Geol* 242:169–190
- Hippensteel SP, Martin RE (1999) Foraminifera as an indicator of overwash deposits, barrier island sediment supply, and barrier island evolution, Folly Island, South Carolina. *Palaeogeogr Palaeoclimatol* 149:115–125
- Horsfield WT (1975) Quaternary vertical movements in the Greater Antilles. *Geol Soc Am Bull* 86:933–938
- Howard J (1970) Reconnaissance geology of Anegada Island. Caribbean Research Institute, St. Thomas, p 18
- Hughen KA, Baillie MGL, Bard E, Beck JW, Bertrand CJH, Blackwell PG, Buck CE, Burr GS, Cutler KB, Damon PE, Edwards RL, Fairbanks RG, Friedrich M, Guilderson TP, Kromer B, McCormac G, Manning S, Ramsey CB, Reimer PJ, Reimer RW, Remmele S, Southon JR, Stuiver M, Talamo S,



- Taylor FW, van der Plicht J, Weyhenmeyer CE (2004) Marine04 marine radiocarbon age calibration, 0–26 cal kyr BP; IntCal04; calibration. *Radiocarbon* 46:1059–1086
- Jarecki L, Walkey M (2006) Variable hydrology and salinity of salt ponds in the British Virgin Islands. *Saline Syst* 2. doi: [10.1186/1746-1448-2-2](https://doi.org/10.1186/1746-1448-2-2)
- Jones B, Hunter IG (1992) Very large boulders on the Coast of Grand Cayman: the effects of giant waves on rocky coastlines. *J Coast Res* 8:763–774
- Kortekaas S, Dawson AG (2007) Distinguishing tsunami and storm deposits: an example from Martinhal, SW Portugal. *Sediment Geol* 200:208–221
- Lopez AM, Stein S, Dixon T, Sella G, Calais E, Jansma P, Weber J, LaFemina P (2006) Is there a northern Lesser Antilles forearc block? *Geophys Res Lett* 33. doi: [10.1029/2005GL025293](https://doi.org/10.1029/2005GL025293)
- Machado AJ, Moraes SS (2002) A note on the occurrence of the encrusting foraminifera *Homotrema rubrum* in reef sediments from two distinctive hydrodynamic settings. *Ann Brazilian Acad Sci* 74:727–735
- MacKenzie FT, Kulm LD, Cooley RL, Barnhart JT (1965) *Homotrema rubrum* (Lamarck), a sediment transport indicator. *J Sed Res* 35:265–272
- Mamo B, Strotz L, Dominey-Howes D (2009) Tsunami sediments and their foraminiferal assemblages. *Earth-Sci Rev* 96:263–278
- McCann W, Feldman L, McCann M (1984) Catalog of felt earthquakes for Puerto Rico and neighboring islands 1492–1899 with additional information for some 20th century earthquakes. Unpublished material provided as a pdf by the lead author, pp 122
- Millás JC, Pardue L (1968) Hurricanes of the Caribbean and adjacent regions, 1492–1800. Academy of the Arts and Sciences of the Americas, Miami, Fla
- Morton RA, Gelfenbaum G, Jaffe BE (2007) Physical criteria for distinguishing sandy tsunami and storm deposits using modern examples. *Sediment Geol* 200:184–207
- Murray JW (1991) Ecology and palaeoecology of benthic foraminifera. Longman, Harlow, p 397
- O’Loughlin KF, Lander JF (2003) Caribbean tsunamis: a 500-year history from 1498–1998. Kluwer Academic, Dordrecht, Boston, p 263
- Park LE, Siewers FD, Metzger T, Sipahioglu S (2009) After the hurricane hits: recovery and response to large storm events in a saline lake, San Salvador Island, Bahamas. *Quat Int* 195:98–105
- Pickering VW (1983) Early history of the British Virgin Islands: from Columbus to emancipation. Falcon Publications International, pp 248
- Poag CW (1981) Ecologic atlas of benthic foraminifera of the Gulf of Mexico. Marine Science International, Woods Hole, MA
- Reid HF, Taber S (1920) The Virgin Islands earthquakes of 1867–1868. *Bull Seismol Soc Am* 10:9–20
- Reimer PJ, Baille MGL, Bard E, Bayliss A, Beck JW, Bertrand CJH, Blackwell PG, Buck CE, Burr GS, Cutler KB, Damon PE, Edwards RL, Fairbanks RG, Friedrich M, Guilderson TP, Hogg AG, Hughen KA, Kromer B, McCormac G, Manning S, Ramsey CB, Reimer RW, Remmele S, Southon JR, Stuiver M, Talamo S, Taylor FW, van der Plicht J, Weyhenmeyer CE (2004) IntCal04 terrestrial radiocarbon age calibration, 0–26 cal kyr BP; IntCal04; calibration. *Radiocarbon* 46:1029–1058
- Reinhardt EG, Pilarczyk JE, Brown A (2011) Probable tsunami origin for a shell and sand sheet from marine ponds on Anegada, British Virgin Islands. *Nat Hazards*. doi: [10.1007/s11069-011-9730-y](https://doi.org/10.1007/s11069-011-9730-y)
- Sambridge M, Braun J, McQueen H (1995) Geophysical parametrization and interpolation of irregular data using natural neighbors. *Geophys J Int* 122:837–857
- Scott DB, Collins ES, Gayes PT, Wright E (2003) Records of prehistoric hurricanes on the South Carolina coast based on micropaleontological and sedimentological evidence, with comparison to other Atlantic Coast records. *Geol Soc Am Bull* 115:1027–1039
- Stein S (1982) Subduction seismicity and tectonics in the Lesser Antilles Arc. *J Geophys Res* 87:8642–8664
- van Hengstum PJ, Reinhardt EG, Boyce JI, Clark C (2007) Changing sedimentation patterns due to historical land-use change in Frenchman’s Bay, Pickering, Canada: evidence from high-resolution textural analysis. *J Paleolimnol* 37:603–618
- Wei Y, ten Brink US, Atwater BF (2010) Modeling of tsunamis and hurricanes as causes of the catastrophic overflow of Anegada, British Virgin Islands, between 1650 and 1800: Abstract OS42B-03. Presented at 2010 Fall meeting, American Geophysical Union, San Francisco, California, 13–17 December 2010
- Zahibo N, Pelinovsky E, Yalciner AC, Kurkin A, Koselkov A, Zaitsev A (2003) The 1867 Virgin Island Tsunami. *Nat Hazards Ear Sys Sci* 3:367–376